IEEE Access
Multidisciplinary ⋮ Rapid Review ⋮ Open Access Journal

Received May 3, 2022, accepted May 16, 2022, date of publication May 20, 2022, date of current version May 26, 2022.

Digital Object Identifier 10.1109/ACCESS.2022.3176720

Ultra-Miniaturized Antenna for Deeply Implanted Biomedical Devices

NAEEM ABBAS[1], ABDUL BASIR[2], (Member, IEEE), AMJAD IQBAL[3], (Member, IEEE), MUHAMMAD YOUSAF[1], ADEEL AKRAM[1], AND HYOUNGSUK YOO[2], (Senior Member, IEEE)

[1]ACTSENA Research Group, Telecommunication Engineering Department, University of Engineering and Technology, Taxila, Taxila 47050, Pakistan
[2]Department of Electronic Engineering, Hanyang University, Seoul 04763, South Korea
[3]National Institute for Scientific Research (INRS), Montréal, QC H5A 1K6, Canada

Corresponding author: Hyoungsuk Yoo (hsyoo@hanyang.ac.kr)

This work was supported by the National Research Foundation of Korea (NRF) Grant by the Korean Government through the Ministry of Science and ICT (MSIT) under Grant 2022R1A2C2003726.

ABSTRACT A small antenna system plays a vital role in wireless communication and monitoring of key-signs through information collected by implantable devices. Therefore, this study presents an ultra-miniaturized antenna for deeply medical implants, operating at 2.45 GHz industrial, scientific, and medical (ISM) band. To achieve a miniaturized geometry, slotted ground plane and patch, a thin substrate, and a superstrate are used. A liquid crystalline polymer material (Rogers ULTRALAM; $\tan\delta = 0.0025$ and $\epsilon_r = 2.9$) is used as the substrate and superstrate. The proposed antenna has a surface area of 6×6.5 mm^2 and a thickness of 0.2 mm. A realistic device-like environment and analysis in different implantation (homogeneous and heterogeneous + in different organs) sites are used to check and extend the applicability in realistic multiple implanted applications. To ensure the reliability of the communication, link budget is analyzed, which shows that the antenna can successfully communicates up to twenty meters. The proposed antenna has an impedance (10-dB) bandwidth of 480 MHz and peak realized gain of -16.5 dBi in homogeneous phantom. Further, to check the compliance with IEEE C905.1-2005 safety limits, the specific absorption rate is analyzed and found 185.56, 170.24, 134.5, and 124.2 W/kg., which limits with the radiated powers of the antenna to 9.21, 8.56, 10.54, and 12.48 mW in small intestine, large intestine, stomach, and heart, respectively. Finally, the antenna is fabricated and performed *in-vitro* measurements by placing the integrated antenna inside minced pork. The measured results confirm the trends of the simulated results. The proposed antenna exhibits quasi-omnidirectional radiation patterns in both planes. The analysis confirm that the proposed antenna is suitable for deeply implanted biomedical devices such as leadless pacemakers and wireless capsule endoscopes.

INDEX TERMS Implantable antenna, ultra-miniaturized structure, leadless pacemaker, wireless capsule endoscopy, wide bandwidth, high gain, specific absorption rate.

I. INTRODUCTION

Implantable biomedical devices can improve the quality of human life by providing modern healthcare. Hence, researchers have focused on developing high-quality implantable biomedical devices that can be used for many healthcare applications, such as wireless capsule endoscopy, leadless cardiac pacemakers, intracranial pressure monitoring, intra-oral tongue drive systems, and brain and spinal cord stimulators [1]–[4]. It is essential to develop biomedical and electronic devices integrated with the latest technologies for healthcare purposes [4]–[6].

Different frequency bands are used to transmit and receive monitored data using continuous wireless communication with an external system. The MedRadio (401–406 MHz) and ISM (900, 2400 MHz) bands are widely used for wireless communication in medical devices [6]–[10]. Low-frequency bands provide a long communication range and a low specific absorption rate (SAR); however, these bands cannot support applications such as capsule endoscopy that require high data rates. Implantable devices that are extremely small and compact and have a high gain can be designed for high-frequency bands [11].

The associate editor coordinating the review of this manuscript and approving it for publication was Giorgio Montisci.

TABLE 1. Antenna designing parameters (Unit:mm).

Parameters	Values	Parameters	Values
H	6	w_2	0.4
W	6.5	d_1	1
h_1	0.8	d_2	0.8
h_2	4.2	d_3	0.6
w_1	2.1	-	-

Designing antenna for deeply implanted devices including wireless capsule endoscopes, is extremely challenging. The properties of human organs change when the capsule is ingested into the gastrointestinal (GI) tract, which has an adverse effect on the performance and properties of implantable antennas [5]. A 9.8 mm^3 implantable antenna operating in the ISM (2.40–2.48 GHz) band with a gain and an impedance bandwidth of −12 dBi and 483 MHz, respectively, was previously designed for GI tract endoscopy [5]. However, this antenna was extremely big to be used in small implants such as wireless leadless pacemakers. An implantable patch antenna was developed for the ISM (2.40–2.48 GHz) band with a 10 dB fractional bandwidth of 20.4 % and a simulated gain of −23 dBi [6]. However, the thickness of the antenna (2 mm) with respect to its overall size (5 mm × 5mm × 2mm) rendered it unsuitable for small implants. An implantable antenna resonating in the ISM band (902–928 MHz) with a large bandwidth of 984 MHz (0.721–1.705 GHz) was also developed for wireless capsule endoscopy [7]. However, it could not be fitted in a leadless pacemaker because it was extremely large. A conformal implantable antenna operating over the MedRadio (401–406 MHz) band was designed for wireless capsule endoscopy [8]. Its simulated gain and bandwidth were satisfactory at −31.5 dBi and 541 MHz, respectively. However, the antenna was large, making it unsuitable for practical wireless endoscopic applications. Another study designed a circularly polarized (CP) implantable antenna with capacitive load for a specialized capsule endoscope. The gain and bandwidth of the antenna were −22 dBi and 190 MHz, respectively. However, it could only be wrapped around devices with diameters ≤ 11 mm. Hence, it could not be used for practical applications such as in Micra pacemakers (leadless pacemakers developed by Medtronic) that have a diameter <7 mm. Moreover, antennas designed by researchers in the past have been application-specific, extremely sensitive to changes in the implantation depth, or extremely large and unsuitable for small devices such as the Micra pacemaker [15]–[21].

To this end, we developed an antenna with a large bandwidth, high gain, low SAR, simple design, and compact size for use in deeply implanted biomedical devices such as wireless capsule endoscopes and leadless pacemakers. The simulated gain and operational bandwidth of the proposed antenna were −16.5 dBi and 480 MHz (2.24–2.72 GHz), respectively, and its volume was 6 × 6.5 × 0.2 mm^3. Furthermore, we investigated all the functional parameters of the proposed antenna such as gain, reflection coefficient, and radiation patterns.

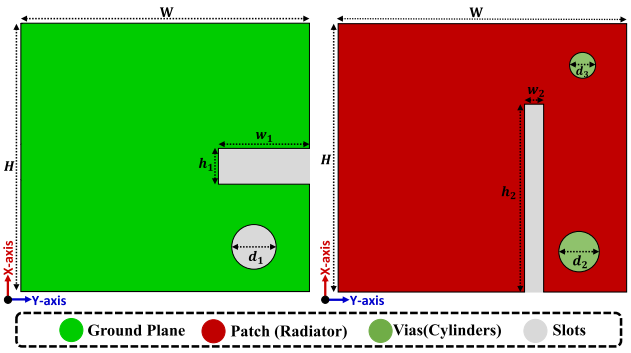

FIGURE 1. Pictorial view of the designed antenna.

II. ANTENNA DESIGN AND PARAMETRIC STUDIES

An implantable antenna is proposed for wireless capsule endoscopy and leadless cardiac pacemaker applications. This study aims to decrease the total volume and SAR and increase the gain and bandwidth of implantable antennas. Various design techniques were first used to minimize the total volume of the proposed antenna.

A. DESIGN PROCESS OF THE PROPOSED ANTENNA

Unlike the free-space, implantable antennas are needed to be optimized in tissue-like environment. To save the time and computing resources, homogeneous phantom of 100 mm × 100 mm × 100 mm, having muscles properties, was selected. Previously, the loops, meandered-line co-planar monopoles and, zigzag-armed dipoles, stacked-patch, and slotted planar inverted-F (PIFA) antennas are previously used for implantable devices. However, PIFAs best suit with ultra-miniaturization techniques. Therefore a rectangular patch antenna patch antenna with dimensions of 6 mm × 6.5 mm × as selected as shown in Figure 1. Such antennas consist of a substrate sandwiched between ground and patch. The operation principles of PIFA antennas are to assign the port between ground and patch where the impedance is 50 Ω while the operating frequency is controlled by the length of the antenna. The optimization of the proposed antenna for the operation frequency of 2.4 GHz was undertaken in four steps as shown in Fig. 2 and their related analysis shown in Figure 3.

Initially, a solid rectangular patch and ground was selected and port and via were placed at the opposite Corners to get the initial resonance. The antenna was resonating at 3.5 GHz but the impedance matching was poor. In second step, an opened-end slot is made on the ground to extend the path trough the port to the via on the ground. The slot on the ground shifted the frequency around 3.2 GHz and improved the matching; however, the matching is still not enough and frequency needs to be shifted toward the targeted frequency of 2.4 GHz. Hence

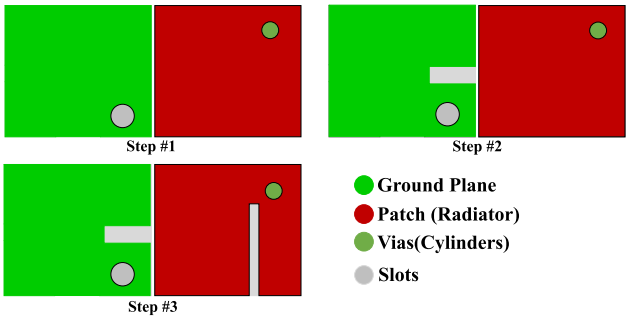

FIGURE 2. Steps followed to design the proposed antenna.

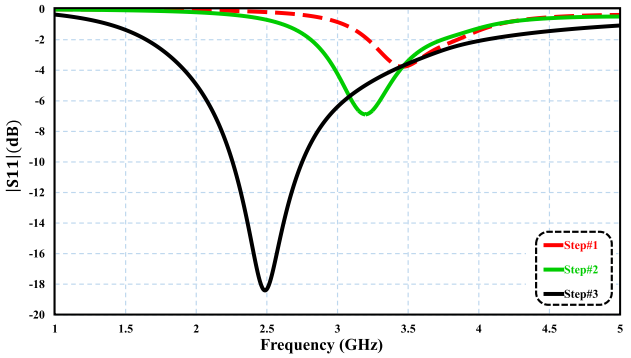

FIGURE 3. The simulated reflection coefficients of the designing step #1, #2, #3.

a slot on the patch, which is perpendicular to the ground slot, is made to optimize the operation frequency to 2.45 GHz. By selecting the accurate lengths of the patch and ground slots the antenna started resonating at 2.45 GHz with a good impedance matching.

The configuration and design of the proposed antenna is very simple to follow. To make the antenna thinner, substrate type and stability are important. Here, the total thickness of the substrate and superstrate is 0.2 mm (each with a thickness of 0.1 mm). Rogers ULTRALAM material is used for fabricating the substrate and superstrate. Its dielectric permittivity and electrical conductivity are $\varepsilon_r = 2.9$ and $\tan\delta = 0.0025$, respectively. Rogers ULTRALAM is a liquid crystalline polymer (LCP) that is widely used for fabricating implantable devices because of its biocompatibility. The dimensions of the antenna are 6 mm $\times$ 6.5 mm $\times$ 0.2 mm. Rectangular slots are created in the ground plane and radiating patch to achieve the required performance. Shorting pins as well as open-ended slots in the ground plane and radiating patch are added to reduce the size of the proposed antenna. The open-ended slot in the radiating patch extends the current on the patch and the return path of the current from the port to the via. The basic parameters of the proposed antenna are listed in Table 1. The center of the proposed antenna is at the origin (0,0). The port of the antenna is located at (2 mm, 2 mm) along the X- and Y-axes. The shorting pin with diameter d_3 is located at (-2 mm, 2 mm) along the X- and Y-axes. The proposed antenna achieves the desired functioning through the desired resonance frequency.

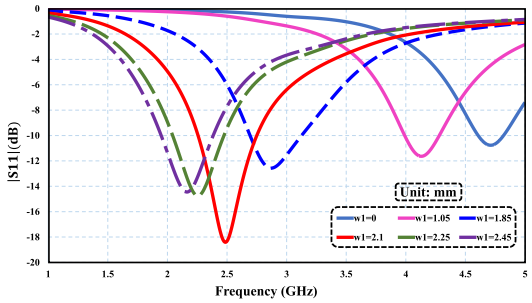

FIGURE 4. Effects of change in slot width (w_1) on the reflection coefficients.

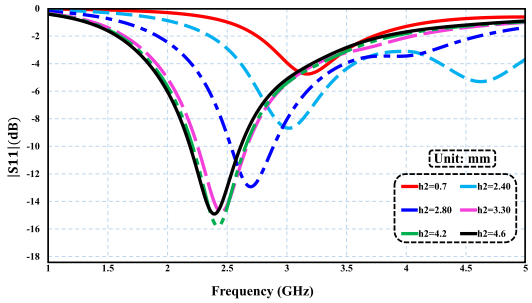

FIGURE 5. Effects of change in slot width (h_2) on the reflection coefficients.

The simulated bandwidth is 480 MHz (2.72–2.24 GHz) covering the 2.45 GHz ISM band, and the simulated gain at the desired frequency is -16.5 dBi.

B. PARAMETRIC STUDY

A parametric study is essential for optimizing the design parameters of the proposed antenna. In this section, three important parameters, w_1, h_2, and the position of the via, were studied to finalize the design of the proposed antenna.

1) CHANGE IN WIDTH w_1 OF THE SLOT IN THE GROUND PLANE

A change in the slot width (w_1) has a significant impact on the reflection coefficient and helps achieve the desired center frequency. The effect of changing the values of w_1 on the reflection coefficient is shown in Fig. 4, where we observe that the resonant frequency changes with a change in w_1. The center frequency increases when the value of w_1 decreases below 2.21 mm and decreases when the value of w_1 increases above 2.21 mm. Therefore, the value of w_1 was fixed at 2.21 mm for obtaining the desired resonant frequency.

2) CHANGE IN LENGTH h_2 OF THE SLOT IN THE RADIATING PATCH

The length of the slot (h_2) in the radiating patch has a significant impact on achieving the resonant frequency. The effect of h_2 on the reflection coefficients is shown in Fig. 5, which indicates that increasing the length of the slot from 0 mm to 3.3 mm reduces the resonant frequency, and impedance matching is achieved for the antenna. Thus, the length of slot h_2 was adjusted to 3.3 mm.

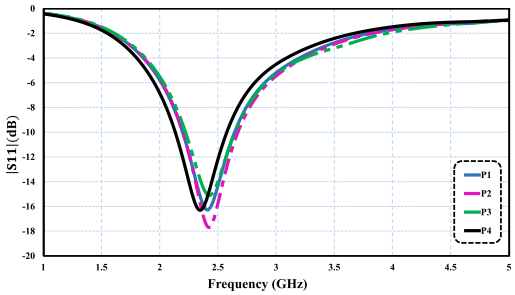

FIGURE 6. Effects of various positions of the via on the reflection coefficients.

TABLE 2. Various positions of shorting pin (via) (Unit:mm).

Parameters	Values (X,Y)	Parameters	Values (X,Y)
P_1	(0,0)	P_4	(-1,-2)
P_2	(-1,-1)	P_5	(1,0)
P_3	(-2,2)		

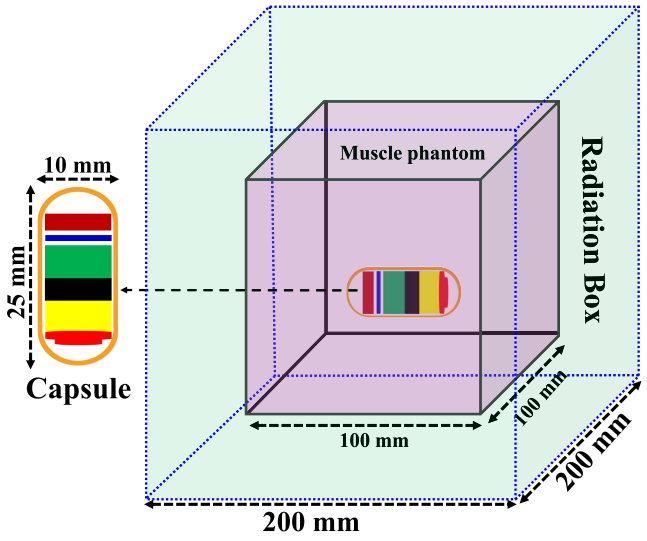

FIGURE 7. Simulation environment for the proposed antenna system.

3) VARIOUS POSITIONS OF THE VIA

The position of the via is important for achieving miniaturization of implantable antennas [10]. The via was moved to different locations to achieve the resonant frequency. The various positions at which the shorting pin (via) was placed are listed in Table 2. The effect of the placement of the via on the reflection coefficients is shown in Fig. 6. As indicated in Fig. 6, changing the location of the shorting pin has no impact on the reflection coefficients. In the proposed antenna, the via was placed at location P_3.

III. SIMULATION SETUP

The simulation setup for the antenna is shown in Fig. 7. The proposed antenna was placed in a homogeneous suscle phantom. The dimensions of the homogeneous muscle phantom are $100 \times 100 \times 100$ mm^3. The electromagnetic properties of small intestine, large intestine, heart, and stomach tissues are listed in Table 3. The $|S11|$ values of the proposed antenna in different human body tissues are shown in Fig. 9, which indicates that the designed antenna covers the 2.45 GHz ISM band in all four tissues. The small intestine tissue disrupts the impedance matching of the antenna owing to its high conductivity. However, the antenna resonates and covers the ISM band. Moreover, the high water content in the stomach increases the permittivity and decreases the resonant frequency in a manageable manner.

TABLE 3. Electromagnetic properties of human body tissues.

Parameters	Permitivity (ε_r)	Conductivity (tanδ)
Small Intestine	54.4	3.17
Large Intestine	53.9	2.04
Stomach	62.2	2.21
Heart	54.8	2.26

A. SYSTEM DEVICE DESIGN FOR THE PROPOSED IMPLANTABLE ANTENNA

The proposed antenna is designed for use in wireless capsule endoscopes and leadless pacemakers. Figure 8 illustrates the integration of the proposed antenna in capsule endoscopes and leadless pacemakers. In the capsule endoscopic device, three batteries are placed and defined as a perfect electric conductor (PEC). A specially designed transceiver is used to transmit and receive electromagnetic signals in the device. The capsule endoscope also includes image sensors, LEDs, and cameras. The housing case of the device system is designed with a biocompatible material, alumina (Al_2O_3). The thickness of alumina is 0.25 mm and its permittivity (ε_r) is 9.8 [11]. The device is then simulated in a homogeneous phantom, the GI tract, and the heart of a human body model. The simulated reflection coefficient values of the designed antenna in different parts of the GUSTAV homogeneous model shown in Fig. 9 confirm that the antenna works effectively in all scenarios. The properties of different tissues (small intestine, stomach, and large intestine) are listed in Table 3. A recoverable change in S_{11} occurred because of the high conductivity of the small intestine and the high permittivity of the stomach due to its high water content.

IV. RESULTS AND DISCUSSION

The proposed antenna was optimized inside a homogeneous phantom using a high-frequency structure simulator (HFSS). The antenna was then simulated in a heterogeneous phantom using CST Microwave Studio. As shown in Fig. 10(a), the antenna is implanted in different parts of the GI tract (such as the small intestine, large intestine, and stomach) and the heart. A comparison of the reflection coefficients of the proposed antenna in the heterogeneous phantoms is shown in Fig. 11. This figure indicates that the proposed antenna covers the 2.45 GHz ISM band. The design and simulations of the antenna were performed using HFSS and CST studio. The observed bandwidth (-10 dB) is 480 MHz

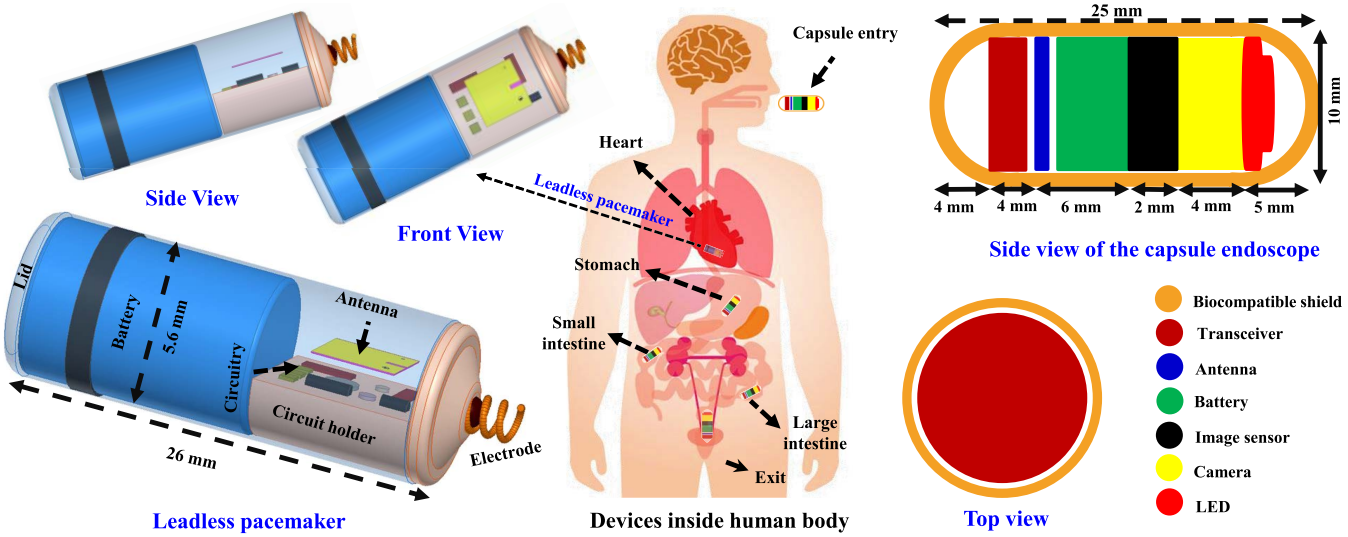

FIGURE 8. Illustrative diagram of wireless data telemetry and monitoring of deep-body implants (leadless pacemaker and capsule endoscope) inside human body.

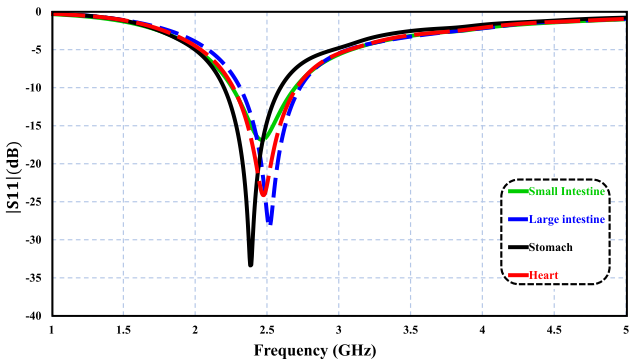

FIGURE 9. Reflection coefficients of the proposed antenna in homogeneous muscle phantoms.

(2.24–2.72 GHz) in the ISM (2.40–2.48 GHz) band. Moreover, the resonance of the antenna shifts to lower frequencies, because the dielectric properties of the stomach are different from those of the large and small intestines.

The radiation patterns (H-plane and E-plane) over the 2.45 GHz ISM band are shown in Fig. 13. The antenna exhibits quasi-omnidirectional radiation patterns, with the simulated and measured patterns showing a high consistency. The deviation in the radiation patterns is primarily because of the asymmetrical operation environments and different conductivity values. The minimum gain peak values obtained in the simulations for the small intestine are owing to its high conductivity, which in turn results in a high energy dissipation in the tissues.

To validate the simulated results, the proposed antenna was fabricated using a chemical etching technique, and the capsule device was fabricated using 3D printing technology, as shown in Fig 10(b). The proposed antenna was placed in minced pork with and without the capsule device, as shown in Figs. 10 (c) and (d), respectively, for testing. The minced pork was placed in a box with a volume of 50 mm $\times$ 100 mm $\times$ 200 mm. To check its radiation patterns, the antenna was also placed in minced pork with and without the capsule device in an anechoic chamber, as shown in Figs. 10 (e) and (f), respectively. The reflection coefficient comparison in different heterogeneous phantoms and the measured results are shown in Fig. 11. As shown in Fig. 11, a high correlation and consistency is observed between the simulated and measured reflection coefficients, and the antenna significantly covers the 2.4 GHz ISM band irrespective of changes in the operation environment.

Posterior to the confirmation of parameters confirmation of the proposed antenna performance such as S-parameters and gain, it is vitally recommended to assess that how long and at what bit rate it can communicate with the external base station. The Friis equations [18] can be used for such analysis to specify the communication ranges of the such devices. In real-time systems, the communication ranges for different implantable applications depends on important parameters such as path loss, transmitter and receiver antenna gains, available radiated power, and data rate. Based on the applications, each implantable device needs a specific data rate limit. Most of the monitoring implants' data rage is limited to a few kilo-bites; however, capsule endoscopes need high data rate to send high resolution images of the GI-tract. Therefore, here we calculated the link-budget for worst case (capsule endoscope). The parameters of the link-budget analysis are tabulated in in Table 5. The transmit power of the implantable devices is limited to -16 dBm in order to comply with the safety limits regulations by the European Research Council.

The basic aim of the link budget analysis is to assess that how long the implantable device can seamlessly communicate through our proposed antenna external monitoring unit. Hence we selected a mononopole as a receiver antenna with a characteristic gain (G_a) of 2.15 dBi. Guaranteed

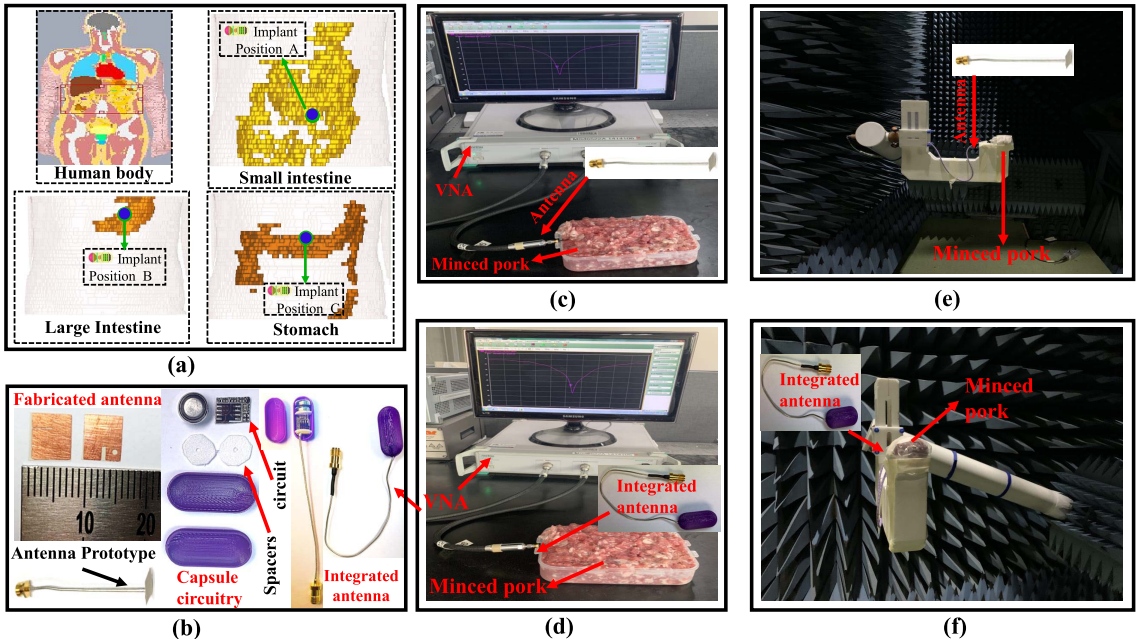

FIGURE 10. Measurement and simulation environments. (a) Different implant positions in the duke human body model. (b) Fabricated and integrated antenna with dummy capsule circuitry. (c) Measurement setup for the reflection coefficient of the fabricated antenna in minced pork. (d) Measurement setup for the reflection coefficient of the integrated antenna with capsule in minced pork. (e) Measurement setup for the gain of the fabricated antenna in minced pork.(f) Measurement setup for the gain of the integrated antenna with capsule in minced pork.

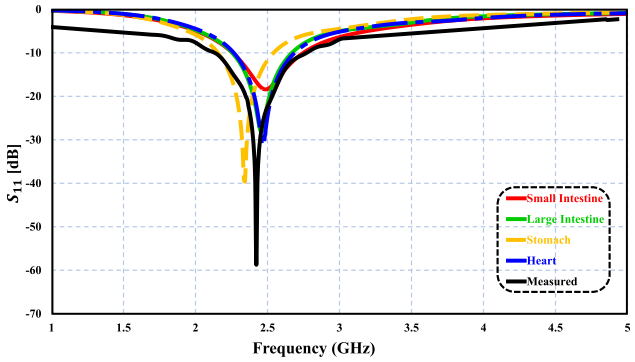

FIGURE 11. Comparison between simulated and measured reflection coefficients.

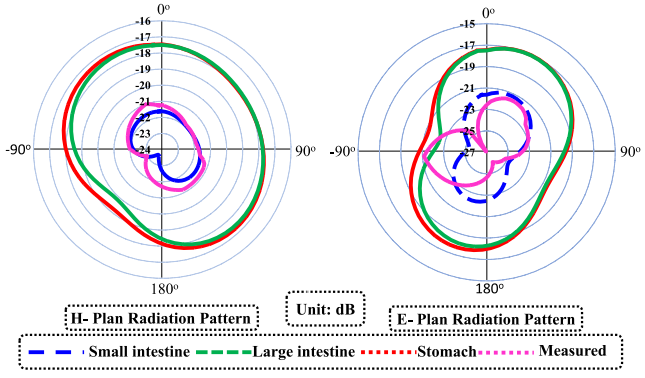

FIGURE 12. H-plan and E-paln radiation patterns.

communication is can be realise through link-margin, which means that if calculated available received power (link

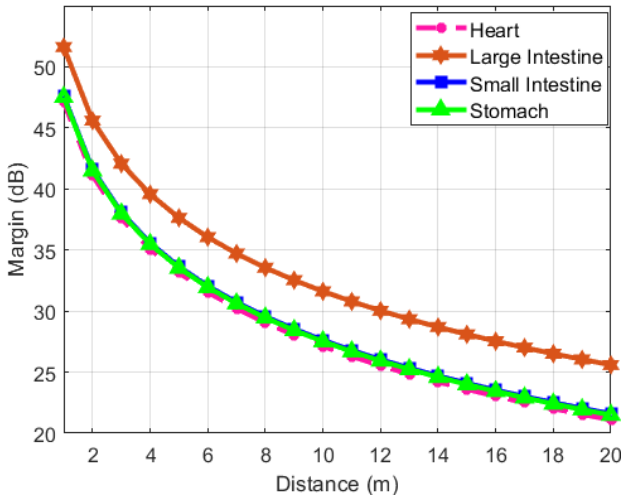

FIGURE 13. Link budget analysis of the antenna in homogeneous phantoms.

budget) A_p is higher than the sensitivity R_p of the receiver device the communication is ensured and seamless. The link margin is calculated through the Friis equations, used in [18], as following.

$$A_P\,(dB/Hz) = P_a + G_a + G_b - L - L_{TxF} - L_{RxF} - N_0 \quad (1)$$

$$R_p\,(dB/Hz) = E_b/N_0 + 10\,log_{10}(B_r) - G_x - G_y \quad (2)$$

where, P_a and G_a are available Tx power and implantable antenna gain; G_b is receiver antenna gain, L is path loss; L_{TxF} and L_{RxF} are transmitter and receiver antenna feeding losses;

TABLE 4. Comparison with the previous work.

Ref	Volume $[mm^3]$	Frequency [GHz]	SAR (W/Kg) 1-g	Bandwidth [MHz]	Gain [dBi]	Dielectric Material	Patch Shape	Shorting Pin
[9]	161.29	2.45	213	190	-22	Rogers 3010	Rectangular	No
[11]	254	2.45	382	60	-15	Roger 3210	Pi-Shape	Yes
[12]	21	2.45	217.849	890	-20.47	Rogers RT/ Duroid 6010	Zig Zag	No
[13]	91.75	2.45	-	300	-17	Rogers 3210	Circular	No
[14]	67.8	2.45	238.9	980	-19.2	Rogers 3010	Rectangular	Yes
[15]	434.65	2.45	350	440	-15.8	Rogers 6010LM	Spiral	Yes
[16]	203.6	0.915	679.797	40	-16	Rogers RO3010	Meandered	Yes
[17]	127	2.45	254.74	390	-17.2	Rogers 3010	Waffel	No
Proposed Work	7.8	2.45	185.56	480	-16.5	Rogers ULTRALAM	PIFA	Yes

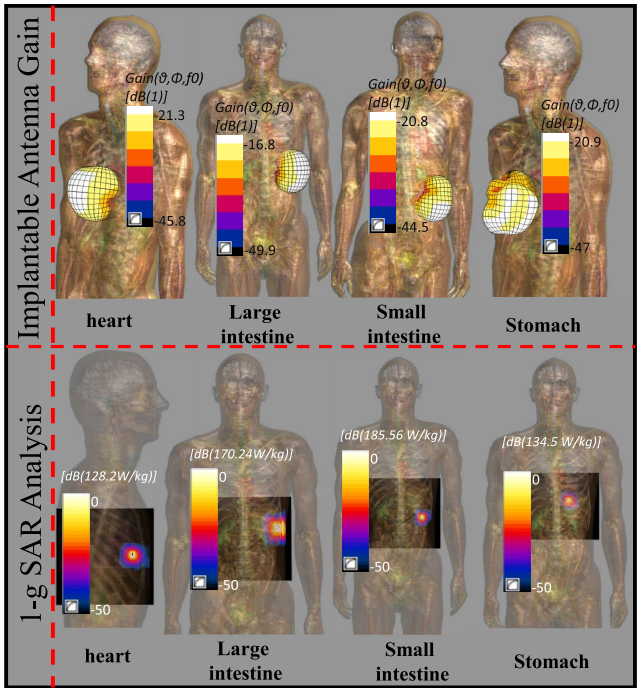

FIGURE 14. 3D-gain and specific absorption rate analysis in heart, stomach, small intestine, and large intestine of the realistic human duke model.

and G_x and G_y are modulation losses, respectively. L is path loss and is given as.

$$L(dB) = 20\ log_{10}(\frac{4\pi d}{\lambda}) \tag{3}$$

$$N_0(dB) = 10\ log_{10}(k) + 10\ log_{10}(T) \tag{4}$$

$$T(K) = T_0(NF - 1) \tag{5}$$

in the above equations d is distance between transmitter and receiver antennas, N_o is noise density and T is temperature. The required link margin parameters are listed in Table 5 and the link-margin for implantable devices with the proposed antenna is shown in Fig. 14 for different applications based on its implantation site. It is obvious from the figure that the link-margin for the proposed antenna is higher than 20 dB with a high data rate of 78 Mb/s, which ensures a reliable

TABLE 5. Link budget parameters.

Symbol	Quantity	Bit Rate (78 Mbps)
P_a	Transmitter power (dBm)	-16
N_o	Noise power density:(dB/Hz)	-20.93
T	Temperature (Kelvin)	310
f	Resonating frequency	2.45 GHz
G_a	Transmitter antenna gain (dBi)	Tissue dependent
G_b	Receiver antenna gain (dBi)	2
L	Free space loss (dB)	Distance dependent
A_P	Available power (dB)	Distance dependent
R_P	Required power (dB)	-155.9
A_p -R_p	Margin (dB)	Fig. 14

communication of the implant during its operation in the range of the external monitoring device.

A. SAR ANALYSIS AND TISSUE EFFECTS

The implantation scenario affecting the performance of the implantable antenna. Basically, the conductivity and permittivity of the tissues and implantation depth plays key role. The permittivity of the implantation site has adverse affect on the matching of the antenna and if the deviation of permittivities of different implantation sites are too high then it can cause a serious shift in the operation frequency. However, in our case, the proposed antenna is simulated in homogeneous tissue phantom and heart, stomach, small intestine and large intestine of realistic Haman model. All these phantoms have comparable values of permittivity and our antenna has a comparatively large bandwidth, therefore there no effects of change in implantation site on |S11| of our proposed antenna. Nonetheless, the conductivity and depth of the implantation site affect the gain of the implantable antennas. The gain has inverse relations conductivity and implantation depth. The 3D gains of the proposed antenna in different organs of the human Duke model are presented in Fig. 13. Although the deviation in peak gain is not too big but still the antenna gain is affected due to tissue effects. From the figure it is obvious that the direction of maximum gain is out of the body, which is required for seamless communication.

To assess the human safety of the proposed antenna through the IEEE C95.1-2005 SAR recommendations, SAR

TABLE 6. 1-g peak special SAR and maximum allowable power at ISM (2.45 GHz) band.

Body tissue	Peak SAR(W/kg)	Max allowable input power (mW)
Small Intestine	185.56	9.21
Large Intestine	170.24	8.56
Stomach	134.5	10.54
Heart	128.2	12.48

is calculated using an FDTD-based software (Sim4Life). The SAR limits defined by IEEE are 2 and 1.6 W/kg for 10 g and 1 g tissues, respectively. The SAR distributions, when antenna is implanted in heart, stomach, small intestine, and large intestine, are presented in Fig. 14 (b). The peak 10-g SAR values for heart, stomach, small intestine, large intestine are 128.2, 134.5, 185.56, and 170. 24 W/kg, respectively. Based on these peak SAR values, the maximum allowable transmit powers for the proposed antenna, to comply with human safety, are calculated. The peak SAR and maximum allowable power of the designed antenna are listed in Table 6. In this study, the maximum allowable transmit powers and SARs were calculated on a 10 g tissue using a 1 W input power. Evaluating on the basis of worst case, the maximum peak SAR of 185. 56 W/kg was found in the small intestine, which limits the maximum allowable transmit power of 9.21 mW. This means that the antenna is safe even if transmit power of 9.21 mW. The high value of SAR is resulted by the high conductivity of the small intestine. However, the maximum allowed transmit power of the implant is way lower (25 microWatt), which confirms that the antenna satisfies the safety standards. The results of the safety analysis suggest that the proposed antenna is suitable for deep-tissue-implanted biomedical devices such as in capsule endoscopes and leadless pacemakers. A detailed comparison between the proposed antenna and existing antennas was also conducted in this study. Table 4 indicates that the proposed antenna has several advantages including a small size, reasonable bandwidth, acceptable gain, and low SAR over other existing antennas.

V. CONCLUSION

A novel ultra-miniaturized antenna with rectangular slots is designed for deep-tissue-implanted capsule endoscopes and leadless pacemakers. The antenna operates in the 2.45 GHz ISM band and is extremely compact ($6 \times 6.5 \times 0.2$ mm^3). A shorting pin and rectangular slots in the ground plane and a radiating patch are used to achieve miniaturization of the antenna. The antenna is simulated and tested in different environments to ensure its in-band operation in various implantation sites. The simulated gain and bandwidth for the proposed antenna are -16.5 dBi and 480 MHz, respectively. The proposed antenna has an omnidirectional radiation pattern with a bandwidth that is sufficient for the required applications. The SAR of the antenna is within the limits specified by IEEE standards. Moreover, when the antenna was placed in different devices in different orientations to check the impact on its functioning, no significant effect was observed. Thus, the proposed antenna is considered to be suitable for deep-tissue-implanted biomedical devices such as capsule endoscopes and leadless pacemakers.

ACKNOWLEDGMENT

(Naeem Abbas and Abdul Basir are co-first authors.)

REFERENCES

[1] Z. Duan and L.-J. Xu, "Dual-band implantable antenna with circular polarisation property for ingestible capsule application," *Electron. Lett.*, vol. 53, no. 16, pp. 1090–1092, Aug. 2017.
[2] D. Nikolayev, M. Zhadobov, L. L. Coq, P. Karban, and R. Sauleau, "Robust ultraminiature capsule antenna for ingestible and implantable applications," *IEEE Trans. Antennas Propag.*, vol. 65, no. 11, pp. 6107–6119, Nov. 2017.
[3] I. A. Shah, M. Zada, and H. Yoo, "Design and analysis of a compact-sized multiband spiral-shaped implantable antenna for scalp implantable and leadless pacemaker systems," *IEEE Trans. Antennas Propag.*, vol. 67, no. 6, pp. 4230–4234, Jun. 2019.
[4] A. Kiourti, K. A. Psathas, and K. S. Nikita, "Implantable and ingestible medical devices with wireless telemetry functionalities: A review of current status and challenges," *Bioelectromagnetics*, vol. 35, no. 1, pp. 1–15, Jan. 2015.
[5] Z. Bashir, M. Zahid, N. Abbas, M. Yousaf, S. Shoaib, M. A. Asghar, and Y. Amin, "A miniaturized wide band implantable antenna for biomedical application," in *Proc. UK/China Emerg. Technol. (UCET)*, Aug. 2019, pp. 1–4.
[6] T. M. Neebha and M. Nesasudha, "Analysis of an ultra miniature capsule antenna for gastrointestinal endoscopy," *Eng. Sci. Technol., Int. J.*, vol. 21, no. 5, pp. 938–944, Oct. 2018.
[7] Z. Duan, L.-J. Xu, S. Gao, and G. Wen, "Integrated design of wideband omnidirectional antenna and electronic components for wireless capsule endoscopy systems," *IEEE Access*, vol. 6, pp. 29626–29636, 2018.
[8] J. Wang, M. Leach, E. G. Lim, Z. Wang, R. Pei, and Y. Huang, "An implantable and conformal antenna for wireless capsule endoscopy," *IEEE Antennas Wireless Propag. Lett.*, vol. 17, no. 7, pp. 1153–1157, Jul. 2018.
[9] C. Liu, Y.-X. Guo, and S. Xiao, "Capacitively loaded circularly polarized implantable patch antenna for ISM band biomedical applications," *IEEE Trans. Antennas Propag.*, vol. 62, no. 5, pp. 2407–2417, May 2014.
[10] M. Zada and H. Yoo, "A miniaturized triple-band implantable antenna system for bio-telemetry applications," *IEEE Trans. Antennas Propag.*, vol. 66, no. 12, pp. 7378–7382, Dec. 2018.
[11] F.-J. Huang, C.-M. Lee, C.-L. Chang, L.-K. Chen, T.-C. Yo, and C.-H. Luo, "Rectenna application of miniaturized implantable antenna design for triple-band biotelemetry communication," *IEEE Trans. Antennas Propag.*, vol. 59, no. 7, pp. 2646–2653, Jul. 2011.
[12] Z.-J. Yang, L. Zhu, and S. Xiao, "An implantable circularly polarized patch antenna design for pacemaker monitoring based on quality factor analysis," *IEEE Trans. Antennas Propag.*, vol. 66, no. 10, pp. 5180–5192, Oct. 2018.
[13] X. Y. Liu, Z. T. Wu, Y. Fan, and E. M. Tentzeris, "A miniaturized CSRR loaded wide-beamwidth circularly polarized implantable antenna for subcutaneous real-time glucose monitoring," *IEEE Antennas Wireless Propag. Lett.*, vol. 16, pp. 577–580, 2016.
[14] L.-J. Xu, Y.-X. Guo, and W. Wu, "Miniaturized dual-band antenna for implantable wireless communications," *IEEE Antennas Wireless Propag. Lett.*, vol. 13, pp. 1160–1163, 2014.
[15] J. Blauert, Y.-S. Kang, and A. Kiourti, "*In vivo* testing of a miniature 2.4/4.8 GHz implantable antenna in postmortem human subject," *IEEE Antennas Wireless Propag. Lett.*, vol. 17, no. 12, pp. 2334–2338, Dec. 2018.
[16] A. Kiourti, M. Christopoulou, and K. S. Nikita, "Performance of a novel miniature antenna implanted in the human head for wireless biotelemetry," in *Proc. IEEE Int. Symp. Antennas Propag. (APSURSI)*, Jul. 2011, pp. 392–395.
[17] H. Li, Y.-X. Guo, and S.-Q. Xiao, "Broadband circularly polarised implantable antenna for biomedical applications," *Electron. Lett.*, vol. 52, no. 7, pp. 504–506, Mar. 2016.

[18] A. Basir, M. Zada, Y. Cho, and H. Yoo, "A dual-circular-polarized endoscopic antenna with wideband characteristics and wireless biotelemetric link characterization," *IEEE Trans. Antennas Propag.*, vol. 68, no. 10, pp. 6953–6963, Oct. 2020.
[19] M. Zada, I. A. Shah, A. Basir, and H. Yoo, "Ultra-compact implantable antenna with enhanced performance for leadless cardiac pacemaker system," *IEEE Trans. Antennas Propag.*, vol. 69, no. 2, pp. 1152–1157, Feb. 2021.
[20] A. Iqbal, M. Al-Hasan, I. B. Mabrouk, A. Basir, M. Nedil, and H. Yoo, "Biotelemetry and wireless powering of biomedical implants using a rectifier integrated self-diplexing implantable antenna," *IEEE Trans. Microw. Theory Techn.*, vol. 69, no. 7, pp. 3438–3451, Jul. 2021.
[21] A. Basir and H. Yoo, "A quadband implantable antenna system for simultaneous wireless powering and biotelemetry of deep-body implants," in *IEEE MTT-S Int. Microw. Symp. Dig.*, Aug. 2020, pp. 496–499.

NAEEM ABBAS received the B.Sc. degree in telecommunication engineering from the University College of Engineering and Technology (UCET), Islamia University Bahawalpur, Pakistan, in 2018, and the M.Sc. degree in telecommunication engineering from the University of Engineering and Technology (UET), Taxila, Pakistan, in 2021. Currently, he is working on implantable antennas and systems, passive chipless RFID tags, wireless power transfer, wireless communication, the Internet of Things (IoT), and image processing. He is a Registered Member of the Pakistan Engineering Council (PEC).

ABDUL BASIR (Member, IEEE) was born in Khyber Pukhtoonkhwa, Pakistan, in 1989. He received the B.Sc. degree in telecommunication engineering from the University of Engineering and Technology, Peshawar, Pakistan, in 2015, and the Ph.D. degree in electronic engineering from Hanyang University, Seoul, South Korea, in 2021. Currently, he is working as a Postdoctoral Researcher with Hanyang University. His research interests include implantable antennas and systems, biomedical circuits, wearable antennas, MIMO communication, metamaterial, dielectric resonator antennas, reconfigurable antennas, long range wireless power transfer, and wireless charging of biomedical implants. He was awarded the Silver Prize for the 2018 and 2019 Best Student Paper Awards in Student Paper Contests by IEEE Seoul Section. His collaborated paper was awarded with the 2019 Best Paper Award by IEEE AP/MTT/EMC Joint Chapter Malaysia. He is also awarded with the Third Prize for the 2018 Best Student Paper Completion by the Korea Communications Agency (KCA) and the Korean Institute of Electromagnetic Engineering and Science (KIEES).

AMJAD IQBAL (Member, IEEE) received the degree in electrical engineering from COMSATS University, Islamabad, Pakistan, in 2016, and the M.S. degree in electrical engineering from the Department of Electrical Engineering, CECOS University of IT and Emerging Science, Peshawar, Pakistan, in 2018. He worked as a Lab Engineer with the Department of Electrical Engineering, CECOS University, Peshawar, from 2016 to 2018. His research interests include printed antennas, flexible antennas, implantable antennas, MIMO antennas, dielectric resonator antennas, wireless power transfer, and synthesis of microwave components. He was a recipient of the 2019 Best Paper Award by IEEE AP/MTT/EMC Joint Chapter Malaysia.

MUHAMMAD YOUSAF received the B.Sc. degree in electronics engineering from the University of Engineering and Technology (UET), Taxila, Pakistan, in 2014, and the M.Sc. degree in electrical engineering from COMSATS University Islamabad, in 2017. He is currently pursuing the Ph.D. degree with UET Taxila. He is working with the ACTSENA Research Group, UET Taxila, focused on implantable antennas and systems, RF coils, wireless power transfer, image processing, and passive chipless RFID tags.

ADEEL AKRAM received the B.S. degree in electrical engineering from the University of Engineering and Technology at Lahore (CE and ME Campus), Lahore, Pakistan, in 1995, the M.S. degree in computer engineering from the National University of Science and Technology, Rawalpindi, Pakistan, in 2000, and the Ph.D. degree from the University of Engineering and Technology at Taxila, Taxila, Pakistan, in 2007. He is currently the Dean of the Faculty of Telecommunication and Information Engineering, University of Engineering and Technology at Taxila. His research interests include the Internet of Things, pervasive computing, wireless communications, broadband networking, and routing.

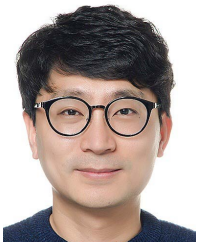

HYOUNGSUK YOO (Senior Member, IEEE) received the B.Sc. degree in electrical engineering from Kyungpook National University, Daegu, South Korea, in 2003, and the M.Sc. and Ph.D. degrees in electrical engineering from the University of Minnesota, Minneapolis, MN, USA, in 2006 and 2009, respectively. In 2009, he joined the Center for Magnetic Resonance Research, University of Minnesota, as a Postdoctoral Associate. In 2010, he joined Cardiac Rhythm Disease Management, Medtronic, MN, USA, as a Senior EM/MRI Scientist. From 2011 to 2018, he was an Associate Professor with the Department of Biomedical Engineering, School of Electrical Engineering, University of Ulsan, Ulsan, South Korea. He has been the CEO of E2MR, a startup company, since 2017. Since 2018, he has been an Associate Professor with the Department of Biomedical Engineering, Hanyang University, Seoul, South Korea. His current research interests include electromagnetic theory, numerical methods in electromagnetics, metamaterials, antennas, implantable devices, and magnetic resonance imaging in high-magnetic field systems. He was awarded the Third Prize for the Best Student Paper at the 2010 IEEE Microwave Theory and Techniques Society International Microwave Symposium.